Fossil chironomid assemblages and inferred summer temperatures for the past 14,000 years from a low-elevation lake in Pacific Canada

J. Lemmen & T. Lacourse

April 2018

Title: Fossil chironomid assemblages and inferred summer temperatures for the past 14,000 years from a low-elevation lake in Pacific Canada

Authors: J. Lemmen and T. Lacourse

Department of Biology, University of Victoria, Victoria, British Columbia, Canada

Corresponding Author:

Terri Lacourse, Dept. of Biology, University of Victoria, Victoria, British Columbia, Canada

Email: tlacours@uvic.ca

Keywords

Chironomidae; *Chaoborus*; Temperature reconstruction; Transfer function; randomTF test; Younger Dryas; British Columbia; Climate change

Abstract

Fossil midge remains in a sediment core from Lake Stowell, a low-elevation lake in coastal British Columbia, Canada, were used to assess temporal changes in chironomid communities and to produce quantitative estimates of mean July air temperature (MJAT) for the past 14,000 years based on two different transfer functions. Chironomid assemblages are diverse throughout much of the record, with most taxa present at low relative abundances. The basal portion of the sediment record is characterized by low head capsule concentrations, taxonomic diversity and organic matter content, all of which increase towards the early Holocene. Inferred temperatures suggest a cool late-glacial interval with a minimum MJAT of 12.5 °C, ~2 °C cooler than the inferred modern temperature. Summer temperatures gradually increased from this minimum until a brief cooling of as much as ~3 °C relative to modern that coincides with the Younger Dryas chronozone. An interval of warmer summers with MJAT of ~16-18 °C (2-3 °C warmer than modern) is inferred between ~10,500 and 8000 cal yr BP. This early Holocene warm period was followed by generally cooler inferred temperatures in the middle and late Holocene. The midge-inferred temperature record from Lake Stowell is generally consistent with other temperature reconstructions from the region based on chironomid remains and other climate proxies. This research underscores the potential of low-elevation, mid-latitude sites for chironomid-based temperature reconstructions. In order to maximize the availability of modern analogues for robust temperature reconstructions from similar sites, calibration datasets should be expanded to include more sites from the warm end of the temperature gradient.

Introduction

Fossil chironomid remains preserved in lake sediments are now used routinely to infer changes in summer air temperature on long ecological timescales. The basis of this approach rests on the fact that the distribution of individual chironomid taxa and therefore the composition of chironomid assemblages are strongly related to air and water temperature (Eggermont and Heiri 2012). Other limnological variables such as dissolved organic carbon and total nitrogen (Medeiros et al. 2015) are also important in controlling the distribution and abundance of chironomid taxa, but the direct and indirect effects of summer temperature plays an overarching role (Eggermont and Heiri 2012; Brooks et al. 2012). The development of modern calibration datasets has allowed this chironomid-temperature relationship to be quantified. In turn, reconstruction of past temperatures has become a central focus of chironomid-based paleoenvironmental studies.

In North America, some of the earliest studies that used fossil chironomids as paleoenvironmental indicators were conducted in British Columbia (e.g. Walker and Mathewes 1987, 1989a). Quantitative reconstructions of July air temperature have now been published for a number of sites in southern British Columbia (Palmer et al. 2002; Rosenberg et al. 2004; Chase et al. 2008). Overall, these studies suggest relatively rapid warming following deglaciation to an early Holocene thermal maximum, followed by cooling through the late Holocene. All of these studies were based on lake sediment records from high-elevation, inland sites, typically near or at treeline. Such sites are regularly the focus of paleoenvironmental studies because treeline environments are particularly sensitive to environmental change (Battarbee et al. 2002; Huber et al. 2005).

Here, we document changes in chironomid communities over the last 14,000 cal yr at a low-elevation lake on Saltspring Island in coastal British Columbia, Canada. We briefly assess the use of *Chaoborus* mandibles as a proxy for past fish presence, and apply two published transfer functions (Barley et al. 2006; Fortin et al. 2015) to the fossil midge assemblages to infer mean July air temperatures for south-coastal British Columbia. We compare the resulting temperature reconstructions to those based on midge records from high-elevation, inland lakes in the region to evaluate the potential for low-elevation, coastal lakes to serve as robust sites for midge-based temperature reconstructions. To assess the reliability of the temperature

reconstructions from Saltspring Island, we tested their statistical significance following Telford and Birks (2011), verified that fossil assemblages had good modern analogues in the calibration datasets, and compared the reconstructions to other paleotemperature records from the region, including those based on proxies other than chironomids.

Study site

Lake Stowell (48°46'54"N, 123°26'38"W) is a small lake on Saltspring Island, the largest island in an archipelago located along the inner coasts of southern British Columbia, Canada and northwest Washington, USA (Fig. 1). The archipelago sits in the rainshadow of the Vancouver Island Ranges and Olympic Mountains, to the west and south, respectively. Based on 1981-2010 climate normals, mean daily air temperatures on Saltspring Island range from 2.8 °C in January to 16.1 °C in July (Environment Canada 2016). Mean annual precipitation is 1070 mm, with most falling as rain between October and April.

During the Last Glacial Maximum, the archipelago was covered by the Juan de Fuca Lobe of the Cordilleran Ice Sheet. Deglaciation began in the region ~17,500 cal yr BP and the archipelago appears to have been mostly ice-free within about two thousand years (Barrie and Conway 2002; Mosher and Hewitt 2004). Relative sea level immediately following deglaciation (~14,350 cal yr BP) was +75 m above present, and then dropped rapidly to a lowstand of up to –30 m at ~11,000 cal yr BP, before reaching levels comparable to the present in the middle Holocene (James et al. 2009).

Lake Stowell is located 1.5 km from the shoreline of Fulford Harbour at 70 m above present sea level. It has a surface area of 5 ha, a maximum depth of 7.5 m, and a small, poorly-defined inflowing stream in its northeastern corner. Limnological measurements in July 2015 included Secchi depth (2.3 m), pH (7.77), conductivity (103 µS/cm), dissolved organic carbon (5.6 mg/L), and total organic carbon (5.8 mg/L). Ormond et al. (2011) recorded low chlorophyll *a* (1.6 µg/L) and phosphorus (7 µg/L), and high dissolved oxygen (90.8% saturation) at Lake Stowell in July 2008. Three species of fish (rainbow trout, cutthroat trout, threespine stickleback) are found in the lake at present. The lake has been stocked with cutthroat and rainbow trout since 1927 and 1974, respectively.

Materials and methods

Field and laboratory methods

A 768.5-cm sediment core was collected from Lake Stowell at a water depth of 7.24 m using a 5-cm-diameter Livingstone piston corer. The sediment-water interface and uppermost 70 cm of sediment were obtained using a clear polycarbonate tube fit with a piston. Loss-on-ignition was used to estimate organic matter content (%) of the sediment (Heiri et al. 2001). Sediment subsamples (1 cm^3) were taken every 3–8 cm, dried at 105 °C for 20 h, and ignited at 550 °C for 4 h. Magnetic susceptibility was measured every 1–2 cm using a Bartington MS2E high-resolution surface scanning sensor.

Six AMS radiocarbon ages (^{14}C yr BP) were obtained on plant macrofossils and calibrated to calendar years (cal yr BP) using the IntCal13 calibration dataset (Reimer et al. 2013). A chronology based on these ages, the Mazama tephra (Egan et al. 2015), and –63 cal yr BP for the top of the core was built using Stineman interpolation (Stineman 1980) with the 'stinepack' (Johannesson et al. 2012) and 'clam' (Blaauw 2010) packages in R (R Core Team 2016).

Chironomid analysis was conducted on sediment subsamples every 2–6 cm to a depth of 611 cm. Below this depth, sediments were more or less barren of midge remains. Subsample volume varied between 2 and 8.5 cm^3 of sediment, although most samples consisted of 2.5 cm^3. Sediments were prepared using a 5-min treatment of warm 5% KOH and gentle washing through 90-µm mesh using distilled water (Walker 1991). Midge remains were hand-picked using forceps from the >90-µm fraction at 20–40× magnification, with each sample in a Bogorov counting tray, and then transferred to coverslips and mounted on slides with Entellan.

A minimum of 50 complete head capsules were identified per sample, except at 0 cm and 610 cm where this was not possible due to extremely low head capsule concentrations. Midge remains were identified, primarily to genus or morphotype, using a Zeiss A2 compound microscope at 200-630× magnification and following various keys, descriptions and photographs, including Walker (2007), Brooks et al. (2007), Andersen et al. (2013), and Oliver and Roussel (1983). Following Walker (2001), taxa given a 'type' designation indicate identification to a morphotype as opposed to species. Identified head capsules were summed and

are presented as percent composition. Complete head capsules and those with more than half of the mentum or ligula were counted as one head capsule, and head capsules broken along the midline of the median tooth were counted as half. Fragments with less than half of the median tooth or missing the median tooth altogether were considered unidentifiable and were not included in the sum. *Chaoborus* mandibles were identified based on the dichotomous key in Uutala (1990). Each mandible was counted as half of one individual, and data are presented as percentages based on the sum of all identified midge remains and as concentrations i.e., number of individuals/cm^3.

Numerical analyses and paleotemperature reconstructions

Cluster analysis of the chironomid percentage data was based on taxa that accounted for at least 5% of the sum and was conducted using optimal splitting by sum-of-squares after square-root transformation of the data. Binary splitting, CONISS and information content techniques produced similar or identical clusters. Statistical significance of the resulting zones was tested using a broken-stick model (Bennett 1996).

Taxonomic diversity was estimated using Hill's N2, which provides a measure of the effective number of abundant taxa within each sample (Hill 1973). Taxonomic evenness was calculated using Simpson's index, the sum of the squared proportions of taxa in each sample, and the total number of taxa in each sample (Smith and Wilson 1996). Diversity and evenness calculations were performed at a common taxonomic resolution, i.e. genus or morphotype. Thus, these metrics are not equivalent to species diversity, but rather provide generalized measures of changes in taxonomic diversity and evenness through time.

Mean July air temperatures at Lake Stowell were inferred using the Barley et al. (2006) and Fortin et al. (2015) transfer functions. The Barley et al. (2006) calibration dataset includes 145 sites located along a north–south transect from southern British Columbia to Alaska, with additional sites in the Canadian Arctic Archipelago. The Fortin et al. (2015) dataset spans northern North America and consists of the 145 sites in Barley et al. (2016) and an additional 289 sites from across Canada and Alaska, with most sites located north of 55° latitude. The Barley et al. (2006) transfer function is based on identified chironomid head capsules from 63

taxa, whereas the Fortin et al. (2105) transfer function is based on identified chironomid head capsules from 70 taxa, as well as unknown head capsules. July air temperature data for both calibration datasets were obtained from New et al. (2002). In applying these transfer functions to our data, we discovered a systematic error in the estimates of July air temperature for some sites in the Barley et al. (2006) and Fortin et al. (2015) datasets that was related to conversion of coordinates from degrees, minutes and seconds to decimal degrees. These errors were rectified for our study and the correct July air temperature data for these sites were pulled from New et al. (2002). Both transfer functions are based on two-component weighted averaging-partial least squares (WA-PLS) with 9999 bootstraps for cross validation (Barley model: $r^2_{boot} = 0.84$, $RMSEP_{boot} = 1.48$ °C, maximum bias = 4.03 °C; Fortin model: $r^2_{boot} = 0.73$, $RMSEP_{boot} = 1.87$ °C, maximum $bias_{boot} = 2.36$ °C). Fossil assemblages from Lake Stowell were compared to modern assemblages in both training sets using squared chord distances (SCD) in the 'analogue' package (Simpson and Oksanen 2016) in R. SCDs greater than the 5th percentile of this distribution were identified as having poor modern analogues. Statistical significance of the midge-inferred temperatures was tested (α=0.05) against reconstructions from 9999 transfer functions trained on random data using the randomTF test in the 'palaeoSig' package (Telford 2015).

Results

Sediment stratigraphy and chronology

The basal portion of the Lake Stowell sediment core (768.5-604 cm) consists of grey clay with <5% organic matter (Fig. 2). Simple wet mounts of these clays after 10-µm sieving revealed an abundance of halophytic diatoms (e.g. *Thalassiosira*, *Campylodiscus*, *Bacillaria socialis*), indicating deposition in a brackish to nearshore marine environment. Light-brown gyttja with high inorganic content (10-20% LOI) occurs between 604 and 579 cm. Most of the sediment core (579-0 cm) consists of dark brown gyttja. Loss-on-ignition increases gradually, from 25% to 50% in these organic sediments, with a noticeable drop to 11% that corresponds with the Mazama tephra (Fig. 2). Magnetic susceptibility is low in the organic sediments and increases

with depth due to higher inorganic content, reaching 400 SI at 7 m. There is a minor increase in susceptibility associated with the Mazama tephra. Ash-free bulk density is 0.05 g/cm^3, on average, except in the basal clays where it decreases to ~0.03 g/cm^3 (Fig. 2).

An age-depth model (Fig. 3) constructed from six AMS radiocarbon ages on plant macrofossils (Table 1), the established age of the Mazama tephra (Egan et al. 2015), and an age of –63 cal yr BP for the top of the sediment core predicted an age of 14,011 ± 180 cal yr BP for the base of the organic sediments. This age is consistent with sea level reconstructions for the region, which estimate that landscapes at the elevation of Lake Stowell (70 m asl) were exposed by 14,000 cal yr BP (James et al. 2009). Sedimentation rates estimated from the age-depth model are 0.04 cm/cal yr throughout most of the record, but there is an interval of lower rates (0.02 cm/cal yr) between ~5300 and 3000 cal yr BP. Maximum rates of 0.08 cm/cal yr occur in the uppermost sediments.

Chironomid assemblages

Chironomid head capsules were identified in 119 samples spanning the last 14,200 cal yr. The mean time span between samples is 120 cal yr and individual samples represent 10 to 45 cal yr. Cluster analysis identified six statistically significant assemblage zones. The uppermost zone (5b) was deemed a subzone of the larger zone beneath it (5a), based on similarity in composition and because it contains only two samples.

Zone 1: 611 – 571 cm (~14,200–13,170 cal yr BP). The eight samples in this zone correspond with inorganic sediments (<20% LOI, Fig. 2) at the base of the sediment core, and are dominated by taxa in the Tanytarsini tribe, which account for ~40% of the assemblages (Fig. 4). *Dicrotendipes nervosus*-type is consistently present at 10-20%. Zone 1 includes taxa at lower abundances that are found at both warm and cool sites in the calibration datasets. For example, *Sergentia* and *Cricotopus*/*Orthocladius*, typically found at cool sites, and *Glyptotendipes* and *Labrundinia*, typical of warm sites, each account for 5-10%. There is also a peak in *Polypedilum* of 27% at the transition to Zone 2. Head capsule concentrations are relatively low compared to the rest of the sediment core, but increase from 3 head capsules/cm^3 (HC/cm^3) at the base to ~23 HC/cm^3 at the transition to Zone 2 (Fig. 5), as LOI and bulk density also increase (Fig. 2).

Assemblages are generally low in diversity, but show a steady increase from 9 taxa at the base to 16 taxa at ~13,500 cal yr BP (Fig. 5).

Zone 2: 571 – 506 cm (~13,170–11,690 cal yr BP). The 13 samples in Zone 2 are characterized by a continued dominance of Tanytarsini, constituting ~30% of the assemblage, and a continued low-level presence of *Sergentia* and *Cricotopus*/*Orthocladius* (Fig. 4). A single head capsule of *Labrundinia*, which is associated with warm summer temperatures, is present at the beginning of this zone. Pentaneurini and *Parakiefferiella bathophila*-type increase in abundance to 10% and 5%, respectively. Taxonomic diversity continues to increase from the previous zone, to an average of 19 taxa (Fig. 5). Head capsule concentrations are almost double that of the previous zone, with a mean of 37 HC/cm^3 and a peak of ~54 HC/cm^3 between ~12,750 and 12,400 cal yr BP that coincides with above average bulk density (Fig. 2) and increasing diversity (Fig. 5).

Zone 3: 506 – 371 cm (~11,690–8610 cal yr BP). This early Holocene zone consists of 27 samples and is marked by an increase in *Chironomus* to a maximum of 27% and up to 9% *Apedilum* (Fig. 4). Other taxa typical of warm sites (e.g. *Glyptotendipes*, *Pseudochironomus*) also increase in relative abundance, including *Cryptotendipes*, which appears for the first time. *Labrundinia* reappears at 10,500 cal yr BP and is more or less consistently present (<6%) for the remainder of the record. *Sergentia* occurs only sporadically. Head capsule concentrations decrease from the previous zone to a relatively stable mean of 25 HC/cm^3 and there is a corresponding decrease in diversity (Fig. 5). In general, assemblages are moderately diverse and even.

Zone 4: 371 – 174 cm (~8610–3390 cal yr BP). Zone 4 is the largest zone with 39 samples. Like Zone 3, assemblages are dominated by Tanytarsini and *Chironomus*, which reaches 45% at 5600 cal yr BP, coincident with a peak in head capsule concentrations (Figs. 4 and 5). *Einfeldia* is at its most abundant, increasing to a maximum of 14% at 6200 cal yr BP. Pentaneurini and *Lauterborniella* are present at 5-10%. *Parakiefferiella bathophila*-type reaches a peak abundance of 16% immediately before the Mazama tephra, and then persists at lower relative abundances for the remainder of the record. A number of other taxa (e.g. *Apedilum*, *Einfeldia*, *Chironomus*) also show marked decreases following deposition of the Mazama tephra. On average, head

capsule concentrations are highest in this zone, with a mean of 42 HC/cm^3 and a maximum concentration of 94 HC/cm^3 at ~5600 cal yr BP (Fig. 5). Diversity in this zone is similar to the previous two zones, with 17 taxa on average; however, assemblages are generally less even because of the abundance of Tanytarsini and *Chironomus* (Figs. 4 and 5).

Zone 5: 174 – 0 cm (~3390 cal yr BP to the present). Zone 5 consists of two statistically significant subzones. Zone 5a contains 30 samples and is characterized by an increase in the total number of taxa present (Fig. 5). Tanytarsini and *Chironomus* generally decrease, but remain abundant (Fig. 4). Pentaneurini occur at frequencies of 10-15% for much of this zone. Taxa that are typical of warm sites in the calibration datasets generally increase (e.g. *Stempellinella*/*Zavrelia*, *Nanocladius*, *Labrundinia*, *Lauterborniella*) with each accounting for 5-10%. Zone 5b consists of the two uppermost samples, which are characterized by a dramatic increase in *Chironomus* to ~60%. Head capsule concentrations gradually decrease towards the present, descending to 7 HC/cm^3 in the two uppermost samples (Fig. 5) of unconsolidated sediment. Taxonomic diversity and evenness are generally high with a maximum diversity of 27 taxa at ~2600 cal yr BP, although the two uppermost samples are low in both diversity and evenness because of the dominance of *Chironomus* (Figs. 4 and 5).

Chaoborus mandibles

Our analysis of *Chaoborus* mandibles in the Lake Stowell sediment core is limited as a consequence of the low concentration of remains (Electronic Supplementary Material [ESM] Fig. S1). Quinlan and Smol (2010) suggested that a representative *Chaoborus* sample can usually be obtained from samples with >40 chironomid head capsules. In all but two of our samples, >50 head capsules were retrieved, and in one of the two samples with <50 head capsules, a total of 79 mandibles were retrieved.

Chaoborus mandibles were found down to a depth of 474 cm (~11,000 cal yr BP), but only occur consistently in the top 109 cm, i.e. the last 1700 cal yr (ESM Fig. S1). In the two uppermost sediment samples, *Chaoborus* mandibles account for 46% and 20% of all midge remains, respectively. Below this, *Chaoborus* mandibles exceed 3% only once. Mandible

concentrations are low with a maximum of only 6 individuals/cm^3, which is comparable to concentrations at some sites (Uutala 1990), but orders of magnitude less than at others (Palm et al. 2012; Tolonen et al. 2012). Mandibles in most samples are either *Chaoborus flavicans* or *C. trivittatus*. *Chaoborus* (*Sayomyia*) occurs sporadically and *C. americanus* was found only in the uppermost 6 cm.

Inferred July temperatures

The Fortin et al. (2015) and Barley et al. (2006) transfer functions yielded similar estimates and changes in July temperatures through time (Fig. 6, ESM Table S1). The two reconstructions have a strong, positive correlation ($r = 0.846$, $p < 0.001$) and differ primarily in the magnitude of inferred temperature change, most notably during the early Holocene. The Fortin model inferred a larger range of temperatures (11.5–18.6 °C) than the Barley model (12.7–15.9 °C). In both cases, RMSEP was substantially lower than the range of inferred temperatures. We also tested a third model by applying the Fortin et al. (2015) transfer function to the 145 sites in the Barley et al. (2006) calibration dataset. Predictably, this model returned results that were intermediate between the other two in all aspects.

In general, both temperature reconstructions infer the lowest temperatures in the most basal samples, i.e. before 13,400 cal yr BP (Fig. 6). Inferred temperatures increase from this late-glacial minimum, until a brief cooling of up to 3 °C, relative to modern, between ~13,000 and 11,800 cal yr BP. This cooling is more pronounced in the Fortin model, in which inferred temperatures reach a record minimum of 11.5 °C, compared to a record minimum of 12.7 °C in the Barley model. Between ~10,500 and 8000 cal yr BP, inferred temperatures increase to 16-18 °C, or up to ~3.7 °C higher than inferred modern temperatures. This early Holocene warm period is followed by generally cooler inferred temperatures in the middle and late Holocene. Both reconstructions suggest a minor increase in temperatures about 2000 cal yr BP.

Significance testing via Telford's (2015) 'randomTF' test indicates that neither model explains a significant amount of variation in the fossil assemblages compared to that explained by reconstructions trained on random environmental variables (Fortin model: $p = 0.320$; Barley model: $p = 0.234$) (Fig. 7). The Fortin model, however, performs well in the modern analogue technique with only 26% of fossil samples having poor analogues in the calibration dataset (Fig.

7A), compared to almost half of all fossil samples (49%) having poor analogues in the Barley model (Fig. 7B). Fossil samples without good modern analogues occur sporadically in the Fortin model, but occur mostly between 12,000 and 9000 cal yr BP in the Barley model, suggesting that the Barley model performs particularly poorly in this interval. Furthermore, the percentage of fossil taxa represented in the two training sets varied considerably. A minimum of 88% of taxa in the individual fossil assemblages are present in the Fortin training set and 71% of fossil samples have all taxa represented. In contrast, a minimum of 76% of taxa in the fossil samples are present in the Barley training set and only 8% of fossil samples have all taxa represented. Taxa that are rare (i.e. with a Hill's N2 of ≤5) in the training sets contribute up to 9% to individual fossil assemblages, but most fossil assemblages (~80%) include 0–2% rare taxa. The Fortin model also has a substantially lower maximum bias (2.36 °C), compared to the Barley model (4.03 °C). Overall, the Barley model does not perform as well as the Fortin model, despite having a slightly lower RMSEP.

Discussion

Midge assemblages at Lake Stowell

Lake Stowell has rich assemblages of chironomids throughout much of its record, with diversity estimates regularly exceeding 18 taxa/sample. Diverse assemblages are typical of modern sediments in low-elevation, temperate lakes (Walker and Mathewes 1989b), but have also been observed in early Holocene sediments at subalpine and high-elevation sites (Palmer et al. 2002; Porinchu et al. 2003). Most taxa are present at low relative abundances at Lake Stowell, a pattern that is typical of other lakes in coastal British Columbia (Walker and Mathewes 1989a). Relatively subtle changes in chironomid community composition through time are in contrast to some higher-elevation, inland lakes in the region (Smith et al. 1998; Palmer et al. 2002; Chase et al. 2008), where more marked changes in composition are observed at times of environmental change.

Much of the Lake Stowell chironomid record is dominated by taxa in the Tanytarsini group, most of which belong to *Tanytarsus*. This group is ubiquitous in western North America,

348 although individual species in this group likely have more restricted ranges. The other dominant
349 taxon, *Chironomus*, is also common in the region, particularly at low- to middle-elevation sites
350 (Walker and Mathewes 1989a). Most *Chironomus* remains at Lake Stowell are *C. anthracinus*-
351 type. Taxa indicative of cold conditions are uncommon in the Lake Stowell record; only
352 *Sergentia* occurs consistently through the late-glacial period. Taxa typical of warm conditions,
353 e.g. *Polypedilum*, *Glyptotendipes*, and *Labrundinia*, which have temperature optima between
354 12.6 and 14.7 °C in the calibration datasets, are also present in late-glacial assemblages.
355 *Chironomus*, which has a temperature optimum of 11.2 °C in the Fortin et al. (2015) dataset,
356 increases markedly after 11,600 cal yr BP. Early Holocene assemblages are also characterized by
357 more subtle increases in taxa associated with warmer temperatures (e.g. *Cryptotendipes*,
358 *Apedilum*, *Lauterborniella*, *Labrundinia*). In middle and late Holocene assemblages, the relative
359 abundance of Tanytarsini decreases and previously infrequent taxa such as *Lauterborniella* and
360 *Stempellinella*/*Zavrelia* increase. The substantial increase in *Chironomus* in the uppermost
361 sediments coincides with increased anthropogenic influence on the lake and surrounding
362 watershed over the last 100 years.
363
364
365 *Chaoborus* as a proxy for fish presence
366
367 The sedimentary remains of *Chaoborus* species have been used in paleolimnological studies as a
368 proxy for fish presence (e.g. Uutala 1990; Lamontagne and Schindler 1994; Uutala and Smol
369 1996; Palm et al. 2012) and even fish biomass and population density (Tolonen et al. 2012). The
370 basis for this approach centers on whether *Chaoborus* species are capable of diurnal migration to
371 avoid predation by fish, which is the case in *C. flavicans* and *C. trivittatus* (Uutala 1990).
372 Although both of these species are found in lakes with fish, they have also been found in fishless
373 lakes (e.g. Lamontagne and Schindler 1994, Garcia and Mittelbach 2008), and therefore cannot
374 be used as definitive indicators of past fish presence.
375 The uppermost sediments at Lake Stowell contain the mandibles of four *Chaoborus*
376 species, most of which are *C. flavicans* or *C. trivittatus*. The prominence of *Chaoborus* species
377 that can avoid predation was expected at Lake Stowell, given that the lake hosts natural and
378 stocked fish populations. *Chaoborus americanus* mandibles, however, were not expected, as this

379 species is regularly reported as being restricted to fishless lakes (Uutala 1990; Walker 2001;
380 Kurek et al. 2010; Quinlan and Smol 2010). The presence of *C. americanus* at Lake Stowell and
381 in other lakes with fish (e.g. Lamontagne and Schindler 1994; Garcia and Mittelbach 2008)
382 suggests this species is not in fact restricted to fishless lakes, and therefore cannot be used to
383 infer the absence of fish. The characterization of lakes into broad categories of fish and fishless
384 using the mandibles of different *Chaoborus* species appears too simplistic to capture the
385 limnological conditions that influence *Chaoborus* populations (Wissel et al. 2003; Quinlan and
386 Smol 2010). Our results suggest that additional research is needed before reliable inferences
387 about past fish presence and abundance can be drawn from *Chaoborus* mandibles alone.
388
389
390 Inferred paleotemperatures at Lake Stowell
391
392 Significance testing of the July air temperature reconstructions using the randomTF test (Telford
393 2015) indicated that neither model was statistically significant; however, this is not uncommon
394 for paleoenvironmental reconstructions based on midges (e.g. Luoto et al. 2014; Upiter et al.
395 2014) and other proxies (e.g. Salonen et al. 2013). Payne et al. (2016) applied the same
396 significance test to 30 reconstructions of water table depth based on testate amoebae and found
397 that only five were statistically significant, with 18 of the remaining reconstructions having *p*-
398 values >0.40. Payne et al. (2016) were unable to identify commonalities among the
399 reconstructions that failed significance testing or among those that passed, and suggested that the
400 test may simply be overly conservative.
401 Poor analogue conditions may be associated with failure of the test, but this does not
402 appear to be a problem with the Lake Stowell reconstruction based on the Fortin et al. (2015)
403 transfer function, for which 74% of the fossil samples have good modern analogues. Telford and
404 Birks (2011) and Luoto et al. (2014) showed that limited variability in reconstructions relative to
405 the training set may lead to non-significant results. This likely explains the results at Lake
406 Stowell: the range of inferred temperatures based on the Fortin et al. (2015) transfer function (i.e.
407 6.5 °C) is substantially lower than the 14.5 °C temperature gradient in this large (n=434)
408 calibration dataset. Non-significant results do not prove that a reconstruction is unreliable, but
409 they do suggest that results should be considered along with other evidence about the reliability

410 of the reconstruction. Given the good performance of the Fortin et al. (2015) transfer function,
411 the availability of modern analogues for the majority of the fossil samples (Fig. 7A), the high
412 representation of fossil taxa in the Fortin training set, and correlations between inferred
413 temperatures and independent records (Fig. 8), it is likely that the non-significant results at Lake
414 Stowell are in fact a Type II error (Telford and Birks 2011; Payne et al. 2016), rather than an
415 indication that the reconstruction is unreliable.
416 Temporal changes in inferred mean July temperatures at Lake Stowell are generally
417 consistent with other midge-based reconstructions from the region (Palmer et al. 2002;
418 Rosenberg et al. 2004; Chase et al. 2008; Gavin et al. 2013). July temperature estimates at Lake
419 Stowell, however, are consistently warmer, which is not surprising since nearby reconstructions
420 are all from inland, subalpine lakes. Changes in temperature at Lake Stowell are also similar to
421 C_{37} alkenone-inferred sea-surface temperature reconstructions (Fig. 8D-F) from sites along the
422 Pacific coast (Barron et al. 2003; Kienast and McKay 2001; Praetorius et al. 2015). Again, Lake
423 Stowell temperature estimates are consistently warmer compared to sea-surface temperature
424 estimates, as would be expected.
425 In the late-glacial period, low elevation areas in south-coastal British Columbia were
426 mostly ice-free by 13,200 cal yr BP (Barrie and Conway 2002) and conifer-dominated forests
427 were well established in the region (Brown and Hebda 2002; Lacourse 2005; Gavin et al. 2013).
428 Our mean July temperature reconstruction suggests a cool late-glacial interval with temperatures
429 of ~13.5 °C, or 1 °C cooler than the inferred modern temperature. This is similar to pollen-based
430 July temperature estimates of ~14°C from Marion Lake (Heusser et al. 1985), which sits at 310
431 m asl, 90 km northeast of Lake Stowell (Site 7 in Fig. 1). Chironomid studies at higher-elevation,
432 inland sites infer cooler temperatures at this time. For example, Chase et al. (2008) report
433 inferred mean July air temperatures of ~8 °C at 1810 m asl in southeastern British Columbia
434 (Site 1 in Fig. 1). As with other paleoenvironmental studies in the region, paleotemperatures at
435 Lake Stowell increase through the late-glacial period towards the Holocene.
436 Increases in inferred temperature are interrupted briefly by cooling of as much as 3 °C
437 relative to modern that coincides with the Younger Dryas chronozone (Fig. 8). Climate model
438 simulations suggest that temporary shutdown of thermohaline circulation in the North Atlantic,
439 associated with freshwater input from the disintegrating Laurentide Ice Sheet, led to cooling
440 throughout the Northern Hemisphere through both atmospheric and oceanic connections

441 (Mikolajewicz et al. 1997; Okumura et al. 2009). Along the North Pacific coast, it is likely that
442 the Aleutian low-pressure system intensified as a result. A Younger Dryas cooling event is
443 recorded in some pollen and foraminiferal records from coastal British Columbia (e.g. Mathewes
444 1993; Lacourse 2005), but others show little to no evidence of cooling at that time (e.g. Lacourse
445 et al. 2005, 2012). Midge-inferred paleotemperature estimates for high-elevation, inland sites
446 (Fig. 8C) suggest that summers were as much as 2.5 °C cooler than present in interior British
447 Columbia during the Younger Dryas chronozone (Gavin et al. 2013). Kienast and McKay (2001)
448 inferred a similar decrease of ~3 °C in sea surface temperatures (Fig. 8E) near the continental
449 slope, approximately 250 km west of Lake Stowell (Site 9 in Fig. 1). Comparable cooling is
450 recorded elsewhere along the Pacific coast (Fig. 8D, F), including a 3 °C cooling to the south, off
451 the coast of northern California (Barron et al. 2003), and a 4 °C cooling to the north, in the Gulf
452 of Alaska (Praetorius et al. 2015).
453 At Lake Stowell, inferred July temperatures regularly exceeded 16 °C between 10,500
454 and 8000 cal yr BP, coincident with maximum summer insolation (Fig. 8A) and warm, dry
455 summers across much of the Pacific Northwest, associated with strengthening of the North
456 Pacific high-pressure system (Heusser et al. 1985; Bartlein et al. 1998; Walker and Pellatt 2003).
457 Early Holocene temperatures at Lake Stowell are higher than midge-inferred temperatures at
458 high-elevation, inland sites in British Columbia (Gavin et al. 2013), but are similar to pollen-
459 based temperature estimates from nearby Marion Lake, which also suggest temperatures >16 °C
460 (Heusser et al. 1985). There is also general agreement in the relative amount of temperature
461 change. At Lake Stowell, early Holocene estimates exceed modern inferred temperatures by 2-3
462 °C (Fig. 8B), and similar differences are observed in midge-based reconstructions (Fig. 8C) from
463 interior British Columbia (Gavin et al. 2013). Sea-surface temperature estimates from the North
464 Pacific (Barron et al. 2003; Kienast and McKay 2001; Praetorius et al. 2015) and oxygen isotope
465 records from the Gulf of Alaska (Praetorius and Mix 2014) and central Greenland (NGRIP 2004)
466 also indicate a warm early Holocene period (Fig. 8D-H). Despite the similarities between
467 inferred early Holocene temperatures at Lake Stowell and other nearby temperature
468 reconstructions, as well as the presence of good modern analogues (Fig. 7A), inferred summer
469 temperatures may well be underestimated. Lake Stowell sits at the warm end of the temperature
470 gradient in the Fortin et al. (2015) calibration dataset and there are only a few sites in the dataset

that are warmer than Lake Stowell. Additional sites from warm climates would help clarify whether early Holocene temperatures at Lake Stowell are indeed underestimated.

In the middle Holocene, summers were cooler along the North Pacific coast (Kienast and McKay 2001; Barron et al. 2003; Praetorius et al. 2015) and across much the Northern Hemisphere (Marcott et al. 2013). Inferred temperatures at Lake Stowell decreased after ~8000 cal yr BP, with estimates fluctuating around 14.6 °C for much of the middle Holocene. This moderate decrease in temperature following the early Holocene is consistent with cooling suggested by most paleoenvironmental studies in the region (Walker and Pellatt 2003), and was likely driven by decreasing summer insolation (Fig. 8A) and intensification of the Aleutian Low (Bartlein et al. 1998).

Most paleoenvironmental records from British Columbia suggest continued cooling or stable temperatures from the middle Holocene to the present (Walker and Pellatt 2003; Kienast and McKay 2001; Gavin et al. 2013). The Lake Stowell temperature reconstruction suggests there may have been a short period of slightly higher temperatures ~2500-1800 cal yr BP. Patterson et al. (2011) reported increasing winter sea-surface temperatures inferred from dinoflagellate cysts at 2300-2200 cal yr BP in nearby Effingham Inlet (Site 8 in Fig. 1), ~130 km northwest of Lake Stowell, and suggested that this may be linked to weakening of the southward flowing California Current that would have facilitated northward movement of warm southern currents up the coast of British Columbia. The dominating effect of ocean circulation patterns on sea surface temperatures would likely also influence near-shore climates such as at Lake Stowell, potentially explaining differences in temperature dynamics between coastal and more continental sites in interior British Columbia. It is also possible that the changes in chironomid assemblages that suggest slightly higher temperatures at ~2000 cal yr BP are instead related to increases in productivity, e.g. higher dissolved organic carbon and/or allochthonous nutrient supply. The temperature reconstruction based on the Barley dataset suggests increasing summer temperatures over the last 100 years, but the reconstruction based on the Fortin dataset does not (Fig. 6). This difference is linked to the abundance of *Chironomus* (Fig. 4), which has a notably higher temperature optimum in the Barley dataset (12.9 °C) compared to the Fortin dataset (11.2 °C). It is likely that the increase in *Chironomus* remains is associated with recent human-induced eutrophication at Lake Stowell, rather than temperature alone.

Conclusions

Fossil chironomid assemblages at Lake Stowell are dominated by Tanytarsini and *Chironomus*; however, assemblages are relatively diverse with many taxa present at low relative abundances. Our research does not support the use of fossil *Chaoborus* mandibles as simple indicators of past fish presence or absence. Additional research is needed in this area.

Despite subtle changes in the composition of chironomid assemblages over the last 14,000 cal yr, the Lake Stowell record suggests notable changes in summer temperature that increase our understanding of paleoenvironmental change on the south coast of British Columbia. Inferred temperatures are coolest in the late-glacial period, but show an increasing trend before decreasing by as much as 3 °C, relative to modern, during the Younger Dryas chronozone. The early Holocene was marked by relatively stable temperatures that exceeded modern by ~2-3 °C. Inferred temperatures generally decrease through the remainder of the Holocene.

Sites selected for inferring past temperatures based on fossil chironomid assemblages are typically located at or near modern ecotones such as treeline, because these sites tend to be sensitive to environmental change. Mean July air temperatures inferred from fossil assemblages at Lake Stowell are more or less consistent with other temperature reconstructions from the region, highlighting the potential for midge-based reconstructions from low-elevation, mid-latitude coastal sites, as others have found (e.g. Whitney et al. 2005; Massaferro et al. 2014). The Fortin et al. (2015) calibration dataset used for the Lake Stowell paleotemperature reconstruction covers large latitudinal and elevational gradients, providing good modern analogues for most of the fossil assemblages. There is a need, however, to expand calibration datasets to include additional modern sites at the warm end of the temperature gradient. This will help ensure that fossil assemblages at low-elevation, mid-latitude sites are well represented by a number of good modern analogues and should further increase the reliability of temperature reconstructions.

Acknowledgements

We thank M. Davies, S. Goring, T. Johnsen, J. Lucas and M. Pellatt for field assistance, D. Fedje for help with diatom identification, I.R. Walker, J. Kurek, A.S. Medeiros and R. Quinlan for help

533 with chironomid identification, and I.R. Walker for constructive comments on a previous version
534 of the manuscript. An anonymous reviewer provided thoughtful feedback that helped improve
535 the manuscript. Funding was provided through research grants to T. Lacourse from the Natural
536 Sciences and Engineering Research Council of Canada, Canada Foundation for Innovation, and
537 Pacific Institute for Climate Solutions.
538
539 **References**
540 Andersen T, Cranston PS, Epler JH (2013) Chironomidae of the Holarctic Region: Keys and
541 Diagnoses. Part 1 Larvae. Insect Syst Evol Suppl 66: 1-571
542
543 Barley EM, Walker IR, Kurek J, Cwynar LC, Mathewes RW, Gajewski K, Finney BP (2006) A
544 northwest North American training set: distribution of freshwater midges in relation to air
545 temperature and lake depth. J Paleolimnol 36: 295-314
546
547 Barrie JV, Conway KW (2002) Rapid sea-level change and coastal evolution on the Pacific
548 margin of Canada. Sediment Geol 150: 171-183
549
550 Barron JA, Heusser L, Herbert T, Lyle M (2003) High-resolution climatic evolution of coastal
551 northern California during the past 16,000 years. Paleoceanography 18: 1020
552
553 Bartlein PJ, Anderson KH, Anderson PM, Edwards ME, Mock CJ, Thompson RS, Webb RS,
554 Webb III T, Whitlock C (1998) Paleoclimate simulations for North America over the past 21,000
555 years: Features of the simulated climate and comparisons with the paleoenvironmental data. Quat
556 Sci Rev 17: 549-585
557
558 Battarbee RW, Thompson R, Catalan J, Grytnes JA, Birks HJB (2002) Climate variability and
559 ecosystem dynamics of remote alpine arctic lakes: the MOLAR project. J Paleolimnol 28: 1-6.
560
561 Bennett KD (1996) Determination of the number of zones in a biostratigraphical sequence. New
562 Phytol 132: 155-170
563

564 Berger A, Loutre MF (1991) Insolation values for the climate of the last 10 million years. Quat
565 Sci Rev 10: 297-317
566
567 Blaauw M (2010) Methods and code for 'classical' age-modelling of radiocarbon sequences.
568 Quat Geochronol 5: 512-518
569
570 Brooks SJ, Axford Y, Heiri O, Langdon PG, Larocque-Tobler I (2012) Chironomids can be
571 reliable proxies for Holocene temperatures. A comment on Velle et al. (2010). Holocene 22:
572 1495–1500
573
574 Brooks SJ, Langdon PG, Heiri O (2007) The Identification and Use of Palaearctic Chironomidae
575 Larvae in Palaeoecology. Technical Guide No. 10. Quaternary Research Association, London
576
577 Brown KJ, Hebda RJ (2002) Origin, development, and dynamics of coastal temperate conifer
578 rainforests of southern Vancouver Island, Canada. Can J For Res 32: 353-372
579
580 Chase M, Bleskie C, Walker IR, Gavin DG, Hu FS (2008) Midge-inferred Holocene summer
581 temperatures in southeastern British Columbia, Canada. Palaeogeogr Palaeoclimatol Palaeoecol
582 257: 244–259
583
584 Egan J, Staff R, Blackford J (2015) A high-precision age estimate of the Holocene Plinian
585 eruption of Mount Mazama, Oregon, USA. Holocene 25: 1054-1067
586
587 Eggermont H, Heiri O (2012) The chironomid-temperature relationship: expression in nature and
588 palaeoenvironmental implications. Biol Rev (Camb): 430–456
589
590 Environment Canada (2016) Canadian Climate Normals, 1981–2010. Meteorological Service of
591 Canada, Environment Canada. (http://climate.weather.gc.ca/climate_normals)
592
593 Fortin M-C, Medeiros AS, Gajewski K, Barley EM, Larocque-Tobler I, Porinchu DF, Wilson SE
594 (2015) Chironomid-environment relations in northern North America. J Paleolimnol 54: 223-237

Garcia EA, Mittelbach GG (2008) Regional coexistence and local dominance in *Chaoborus*: species sorting along a predation gradient. Ecology 89: 1703–1713

Gavin DG, Brubaker LB, Greenwald DN (2013) Postglacial climate and fire-mediated vegetation change on the western Olympic Peninsula, Washington (USA). Ecol Monogr 83: 471-489

Heiri O, Lotter AF, Lemcke G (2001) Loss on ignition as a method for estimating organic and carbonate content in sediments: reproducibility and comparability of results. J Paleolimnol 25: 101–110

Heusser CJ, Heusser LE, Peteet DM (1985) Late-Quaternary climatic change on the American North Pacific Coast. Nature 315: 485-487

Hill MO (1973) Diversity and evenness: a unifying notation and its consequences. Ecology 54: 427-432

Huber UM, Bugmann HKM, Reasoner MA (2005) Global Change and Mountain Regions: An Overview of Current Knowledge. Springer, Dordrecht, Netherlands

James T, Gowan EJ, Hutchinson I, Clague JJ, Barrie JV, Conway KW (2009) Sea-level change and paleogeographic reconstructions, southern Vancouver Island, British Columbia, Canada. Quat Sci Rev 28: 1200–1216

Johannesson T, Bjornsson H, Grothendieck G (2012) stinepack: Stineman, a consistently well behaved method of interpolation. R package version 1.3. (http://cran.r-project.org/package=stinepack)

Kienast S, McKay JL (2001) Sea surface temperatures in the subarctic Northeast Pacific reflect millennial-scale climate oscillations during the last 16 kyrs. Geophys Res Lett 28: 1563–1566

626 Kurek J, Cwynar LC, Weeber RC, Jeffries DS, Smol JP (2010) Ecological distributions of
627 *Chaoborus* species in small, shallow lakes from the Canadian Boreal Shield ecozone.
628 Hydrobiologia 652: 207–221
629
630 Lacourse T (2005) Late Quaternary dynamics of forest vegetation on northern Vancouver Island,
631 British Columbia, Canada. Quat Sci Rev 24: 105-121
632
633 Lacourse T, Delepine JM, Hoffman E, Mathewes RW (2012) A 14,000 year vegetation history of
634 a hypermaritime island on the outer Pacific coast of Canada based on fossil pollen, spores and
635 conifer stomata. Quat Res 78: 572–582
636
637 Lacourse T, Mathewes RW, Fedje DW (2005) Late-glacial vegetation dynamics of the Queen
638 Charlotte Islands and adjacent continental shelf, British Columbia, Canada. Palaeogeogr
639 Palaeoclimatol Palaeoecol 226: 36-57
640
641 Lamontagne S, Schindler DW (1994) Historical status of fish populations in Canadian Rocky
642 Mountain lakes inferred from subfossil *Chaoborus* (Diptera, Chaoboridae) mandibles. Can J Fish
643 Aquat Sci 51: 1376–1383
644
645 Luoto TP, Kaukolehto M, Weckström J, Korhola A, Väliranta M (2014) New evidence of warm
646 early-Holocene summers in subarctic Finland based on an enhanced regional chironomid-based
647 temperature calibration model. Quat Res 81: 50-62
648
649 Marcott SA, Shakun JD, Clark PU, Mix AC (2013) A reconstruction of regional and global
650 temperature for the past 11,300 years. Science 339: 1198-1201
651
652 Massaferro J, Larocque-Tobler I, Brooks SJ, Vandergoes M, Dieffenbacher-Krall A, Moreno P
653 (2014) Quantifying climate change in Huelmo mire (Chile, Northwestern Patagonia) during the
654 Last Glacial Termination using a newly developed chironomid-based temperature model.
655 Palaeogeogr Palaeoclimatol Palaeoecol 399: 214-224
656

Mathewes RW (1993) Evidence for Younger Dryas-age cooling on the north Pacific coast of America. Quat Sci Rev 12: 321-331

Medeiros AS, Gajewski K, Porinchu DF, Vermaire JC, Wolfe BB (2015) Detecting the influence of secondary environmental gradients on chironomid-inferred paleotemperature reconstructions in northern North America. Quat Sci Rev 124: 265-274

Mikolajewicz U, Crowley TJ, Schiller A, Voss R (1997) Modelling teleconnections between the North Atlantic and North Pacific during the Younger Dryas. Nature 387: 384–387

Mosher DC, Hewitt AT (2004) Late Quaternary deglaciation and sea-level history of eastern Juan de Fuca Strait, Cascadia. Quat Int 121: 23–39

NGRIP (2004) High-resolution record of Northern Hemisphere climate extending into the last interglacial period. Nature 431: 147-151

New M, Lister D, Hulme M, Makin I (2002) A high-resolution data set of surface climate over global land areas. Clim Res 21: 1–25

Okumura YM, Deser C, Hu A, Timmermann A, Xie SP (2009) North Pacific climate response to freshwater forcing in the subarctic North Atlantic: ocean and atmospheric pathways. J Climate 22: 1424-1445

Oliver DR, Roussel ME (1983) The Insects and Arachnids of Canada. Part 11. The Genera of Larval Midges of Canada - Diptera: Chironomidae. Agriculture Canada Publication 1746, Minister of Supply and Services, Ottawa, Canada

Ormond CI, Rosenfeld JS, Taylor EB (2011) Environmental determinants of threespine stickleback species pair evolution and persistence. Can J Fish Aquat Sci 68: 1983–1997

687 Quinlan R, Smol JP (2010) The extant *Chaoborus* assemblage can be assessed using subfossil
688 mandibles. Freshw Biol 55: 2458–2467
689
690 Palm F, El-Daoushy F, Svensson J-E (2012) Development of subfossil *Daphnia* and *Chaoborus*
691 assemblages in relation to progressive acidification and fish community alterations in SW
692 Sweden. Hydrobiologia 684: 83–95
693
694 Palmer S, Walker I, Heinrichs M, Hebda R, Scudder G (2002) Postglacial midge community
695 change and Holocene palaeotemperature reconstructions near treeline, southern British Columbia
696 (Canada). J Paleolimnol 28: 469–490
697
698 Patterson RT, Swindles GT, Roe HM, Kumar A, Prokoph A (2011) Dinoflagellate cyst-based
699 reconstructions of mid to late Holocene winter sea-surface temperature and productivity from an
700 anoxic fjord in the NE Pacific Ocean. Quat Int 235: 13–25
701
702 Payne RJ, Babeshko K V, Bellen S Van, Blackford JJ, Booth RK, Charman DJ, Ellershaw MR,
703 Gilbery D, Hughes PDM, Jassey VEJ, Lamentowicz L, Lamentowicz M, Malysheva EA,
704 Mauquoy D, Mazei Y, Mitchell EAD, Swindles GT, Tsyganov AN, Turner TW, Telford RJ
705 (2016) Significance testing testate amoeba water table reconstructions. Quat Sci Rev 138: 131-
706 135
707
708 Porinchu DF, MacDonald GM, Bloom AM, Moser KA (2003) Late Pleistocene and early
709 Holocene climate and limnological changes in the Sierra Nevada, California, USA inferred from
710 midges (Insecta: Diptera: Chironomidae). Palaeogeogr Palaeoclimatol Palaeoecol 198: 403-422
711
712 Praetorius SK, Mix AC (2014) Synchronization of North Pacific and Greenland climates
713 preceded abrupt deglacial warming. Science 345: 444-448
714
715 Praetorius SK, Mix AC, Walczak MH, Wolhowe MD, Addison JA, Prahl FG (2015) North
716 Pacific deglacial hypoxic events linked to abrupt ocean warming. Nature 527: 362-366
717

718 R Core Team (2016) R: a language and environment for statistical computing. R Foundation for
719 Statistical Computing, Vienna, Austria
720
721 Reimer PJ, Bard E, Bayliss A, Beck JW, Blackwell PG, Ramsey CB, Buck CE, Cheng H,
722 Edwards RL, Friedrich M, Grootes PM, Guilderson TP, Haflidason H, Hajdas I, Hatté C, Heaton
723 TJ, Hoffmann DL, Hogg AG, Hughen KA, Kaiser KF, Kromer B, Manning SW, Niu M, Reimer
724 RW, Richards DA, Scott EM, Southon JR, Staff RA, Turney CSM, van der Plicht J (2013)
725 IntCal13 and Marine13 radiocarbon age calibration curves 0-50,000 years cal BP. Radiocarbon
726 55: 1869-1887
727
728 Rosenberg SM, Walker IR, Mathewes RW, Hallett DJ (2004) Midge-inferred Holocene climate
729 history of two subalpine lakes in southern British Columbia, Canada. Holocene 14: 258–271
730
731 Salonen JS, Helmens KF, Seppä H, Birks HJB (2013) Pollen-based palaeoclimate
732 reconstructions over long glacial-interglacial timescales: methodological tests based on the
733 Holocene and MIS 5d-c deposits at Sokli, northern Finland. J Quat Sci 28: 271-282
734
735 Simpson GL, Oksanen J (2016) analogue: analogue and weighted averaging methods for
736 paleoecology. R package version 0.17-0. (http://cran.r-project.org/package=analogue)
737
738 Smith B, Wilson JB (1996) A consumer's guide to evenness indices. Oikos 76: 70-82
739
740 Smith MJ, Pellatt MG, Walker IR, Mathewes RW (1998) Postglacial changes in chironomid
741 communities and inferred climate near treeline at Mount Stoyoma, Cascade Mountains,
742 southwestern British Columbia, Canada. J Paleolimnol 20: 277–293
743
744 Stineman RW (1980) A consistently well-behaved method of interpolation. Creative Computing
745 54-57
746
747 Telford RJ (2015) palaeoSig: Significance tests of quantitative palaeoenvironmental
748 reconstructions. R package version 1.1-3. (http://cran.r-project.org/package=palaeoSig)

Telford RJ, Birks HJB (2011) A novel method for assessing the statistical significance of quantitative reconstructions inferred from biotic assemblages. Quat Sci Rev 30: 1272–1278

Tolonen KT, Brodersen KP, Kleisborg TA, Holmgren K, Dahlberg M, Hamerlik L, Hämäläinen (2012) Phantom midge-based models for inferring past fish abundances. J Paleolimnol 47: 531-547

Upiter LM, Vermaire JC, Patterson RT, Crann CA, Galloway JM, Macumber AL, Neville LA, Swindles GT, Falck H, Roe HM, Pisaric MFJ (2014) Middle to late Holocene chironomid-inferred July temperatures for the central Northwest Territories, Canada. J Paleolimnol 52: 11–26

Uutala AJ (1990) *Chaoborus* (Diptera: Chaoboridae) mandibles – paleolimnological indicators of the historical status of fish populations in acid sensitive lakes. J Paleolimnol 4: 139-151

Uutala AJ, Smol JP (1996) Palaeolimnological reconstructions of long-term changes in fisheries status in Sudbury area lakes. Can J Fish Aquat Sci 53: 174–180

Walker IR (2001) Midges: Chironomidae and related Diptera. In: Smol JP, Birks HJB, Last WM (eds) Tracking Environmental Change Using Lake Sediments, Vol. 4, Zoological Indicators. Kluwer Academic Publishers, Dordrecht, pp 43–66

Walker IR (2007) The WWW field guide to fossil midges. (http://www.paleolab.ca/wwwguide/)

Walker IR, Mathewes RW (1987) Chironomidae (Diptera) and postglacial climate at Marion Lake, British Columbia, Canada. Quat Res 27: 89–102

Walker IR, Mathewes RW (1989a) Early postglacial chironomid succession in southwestern British Columbia, Canada, and its paleoenvironmental significance. J Paleolimnol 2: 1–14

779 Walker IR, Mathewes RW (1989b) Chironomidae (Diptera) remains in surficial lake sediments
780 from the Canadian Cordillera: analysis of the fauna across an altitudinal gradient. J Paleolimnol
781 2: 61–80
782
783 Walker IR, Pellatt MG (2003) Climate change in coastal British Columbia – a
784 paleoenvironmental perspective. Can Water Resour J 28: 531–566
785
786 Whitney BS, Vincent JH, Cwynar LC (2005) A midge-based late-glacial temperature
787 reconstruction from southwestern Nova Scotia. Can J Earth Sci 42: 2051–2057
788
789 Wissel B, Yan ND, Ramcharan CW (2003) Predation and refugia: implications for *Chaoborus*
790 abundance and species composition. Freshw Biol 48: 1421–1431
791

Table 1 AMS radiocarbon ages for Lake Stowell, Saltspring Island, British Columbia

Depth (cm)	Material	Lab Code	Radiocarbon Age (^{14}C yr BP ± 1σ)	Calendar Age Range[a] (cal yr BP)
70–71	*Pseudotsuga menziesii* seed and unidentified plant material	Beta-365557	1040 ± 30	920 – 1050
156–157	*Pseudotsuga menziesii* seed	Beta-353388	2710 ± 40	2750 – 2880
231–232	Unidentified seed	Beta-283076	4880 ± 40	5490 – 5710
330.5–332.5	Mazama tephra	–	–	7580 – 7680 [b]
420–421	Poaceae stem	Beta-353390	8820 ± 40	9700 – 10,150
542	*Nuphar* seed	Beta-353392	10,520 ± 50	12,240 – 12,650
601.5–602	Woody twig	Beta-283077	12,100 ± 60	13,780 – 14,120

[a] 2σ age range rounded to the nearest 10 yr

[b] Egan et al. (2015)

Figure Captions

Fig. 1 Map of southern British Columbia, showing location of Lake Stowell (star) on Saltspring Island and other sites where Holocene temperatures have been inferred from chironomids (1–Windy L. [Chase et al. 2008]; 2–Eagle L. [Rosenberg et al. 2004]; 3–Thunder L. [Chase et al. 2008]; 4–North Crater L. and Lake of the Woods [Palmer et al. 2002]; 5–Cabin L. and 3M Pond [Palmer et al. 2002]; 6–Frozen L. [Rosenberg et al. 2004]), pollen (7–Marion L. [Heusser et al. 1985]), dinoflagellates (8–Effingham Inlet [Patterson et al. 2011]), and C_{37} alkenones (9–[Kienast and McKay 2001])

Fig. 2 Sediment stratigraphy, magnetic susceptibility, loss-on-ignition (550 °C) and ash-free bulk density of the sediment core from Lake Stowell, Saltspring Island. Data below 620 cm are not shown

Fig. 3 Age-depth model for the sediment core from Lake Stowell, Saltspring Island. Grey bands show 95% confidence intervals calculated from 10,000 iterations of Stineman interpolation of the probability distributions of the calibrated radiocarbon ages in Table 1

Fig. 4 Relative abundance of dominant chironomid taxa at Lake Stowell with zonation based on optimal splitting by sum-of-squares. Individual sample depths are shown in the *Tanytarsus* plot. Taxa are arranged left to right from coldest to warmest temperature optima in Fortin et al. (2015). Infrequent taxa are not shown. The dashed line in Zone 4 shows the stratigraphic position of the Mazama tephra

Fig. 5 Lake Stowell chironomid head capsule concentrations, assemblage diversity and evenness. Thick black lines are locally weighted regression lines (lowess, span=0.08)

Fig. 6 Inferred mean July air temperature estimates (±1 standard error) for the Lake Stowell sediment core, based on the two component WAPLS models in Fortin et al. (2015) and Barley et al. (2006), which have RMSEP of 1.87 °C and 1.48 °C, respectively. Smoothed lines are locally weighted regression lines (lowess, span=0.8), which are overlaid in the last panel: thick and thin lines are reconstructions based on Fortin et al. (2015) and Barley et al. (2006), respectively

828

829 **Fig. 7** Modern analogue comparisons of the Lake Stowell chironomid assemblages to the (**A**)
830 Fortin et al. (2015) and (**B**) Barley et al. (2006) calibration datasets, based on square chord
831 distances. In **A** and **B**, vertical lines represent the dissimilarity between Lake Stowell samples
832 and modern sites in the two calibration datasets. Dashed horizontal lines represent the 5th
833 percentile of dissimilarities, separating good and poor modern analogues. In **C** and **D**, histograms
834 show the distribution of variance in the fossil assemblages explained by 9999 transfer functions
835 trained on random data for the (**C**) Fortin et al. (2015) and (**D**) Barley et al. (2006) transfer
836 functions. Thick vertical lines represent the proportion of variance explained by the temperature
837 reconstructions and dashed vertical lines represent the 95% percentile of the null distributions
838

839 **Fig. 8** (**A**) January and July insolation anomalies at 50 °N (Berger and Loutre 1991). (**B**) Midge-
840 inferred mean July air temperature (MJAT) anomalies and lowess smoothing from Lake Stowell
841 (49 °N) based on Fortin et al. (2015). (**C**) Loess smoothing of MJAT anomalies from Gavin et al.
842 (2013), which is based on four midge records from inland, subalpine lakes in southern British
843 Columbia (Palmer et al. 2002; Rosenberg et al. 2004; Chase et al. 2008). (**D**, **E** and **F**) Alkenone-
844 inferred sea surface temperatures (SST) for the northeast Pacific Ocean from marine cores near
845 northern California at 42 °N (Barron et al. 2003), near Vancouver Island at 49 °N (Kienast and
846 McKay 2001), and in the Gulf of Alaska at 59 °N (Praetorius et al. 2015), respectively. (**G**) Gulf
847 of Alaska (59 °N) $\delta^{18}O$ record (Praetorius and Mix 2014). (H) NGRIP (2004) $\delta^{18}O$ record. Grey
848 band marks the Younger Dryas chronozone
849

850 **Electronic Supplementary Material Fig. S1** *Chaoborus* percentages and total concentration
851 (individuals/cm^3) in the sediment core from Lake Stowell, Saltspring Island, British Columbia.
852 Each *Chaoborus* mandible was counted as half of one individual. Note changes in scale for *C.*
853 (*Sayomyia*) and *C. americanus*. Grey shading represents 5× exaggeration
854

855 **Electronic Supplementary Material Table S1** Lake Stowell sample depths, sample ages, and
856 inferred mean July air temperature estimates using the Fortin et al. (2015) and Barley et al.
857 (2006) transfer functions

Figure 1

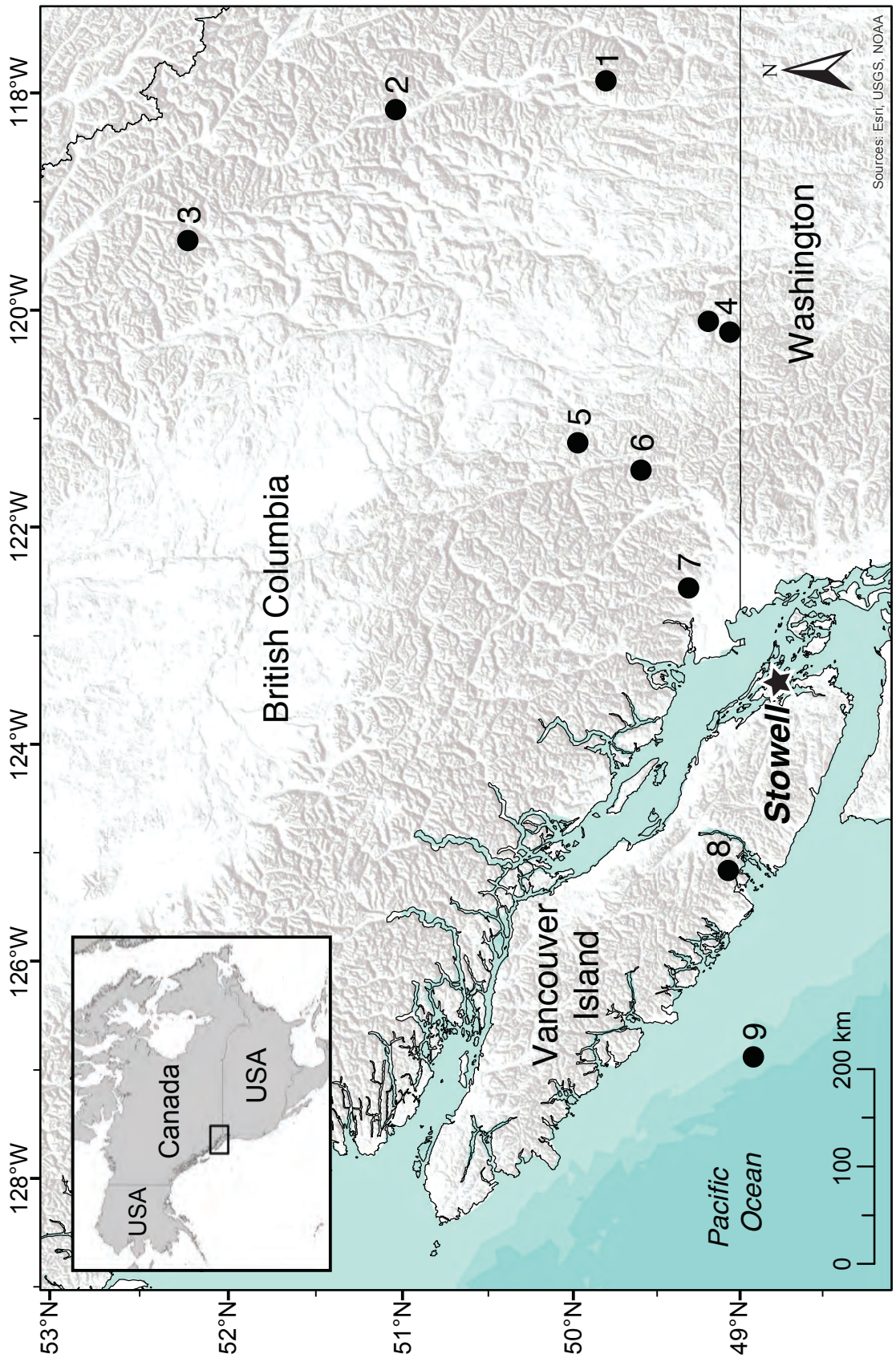
British Columbia
Washington
Vancouver Island
Pacific Ocean
Stowell
1
2
3
4
5
6
7
8
9
USA
Canada
USA
128°W
126°W
124°W
122°W
120°W
118°W
53°N
52°N
51°N
50°N
49°N
0
100
200 km
N
Sources: Esri, USGS, NOAA

Figure 2

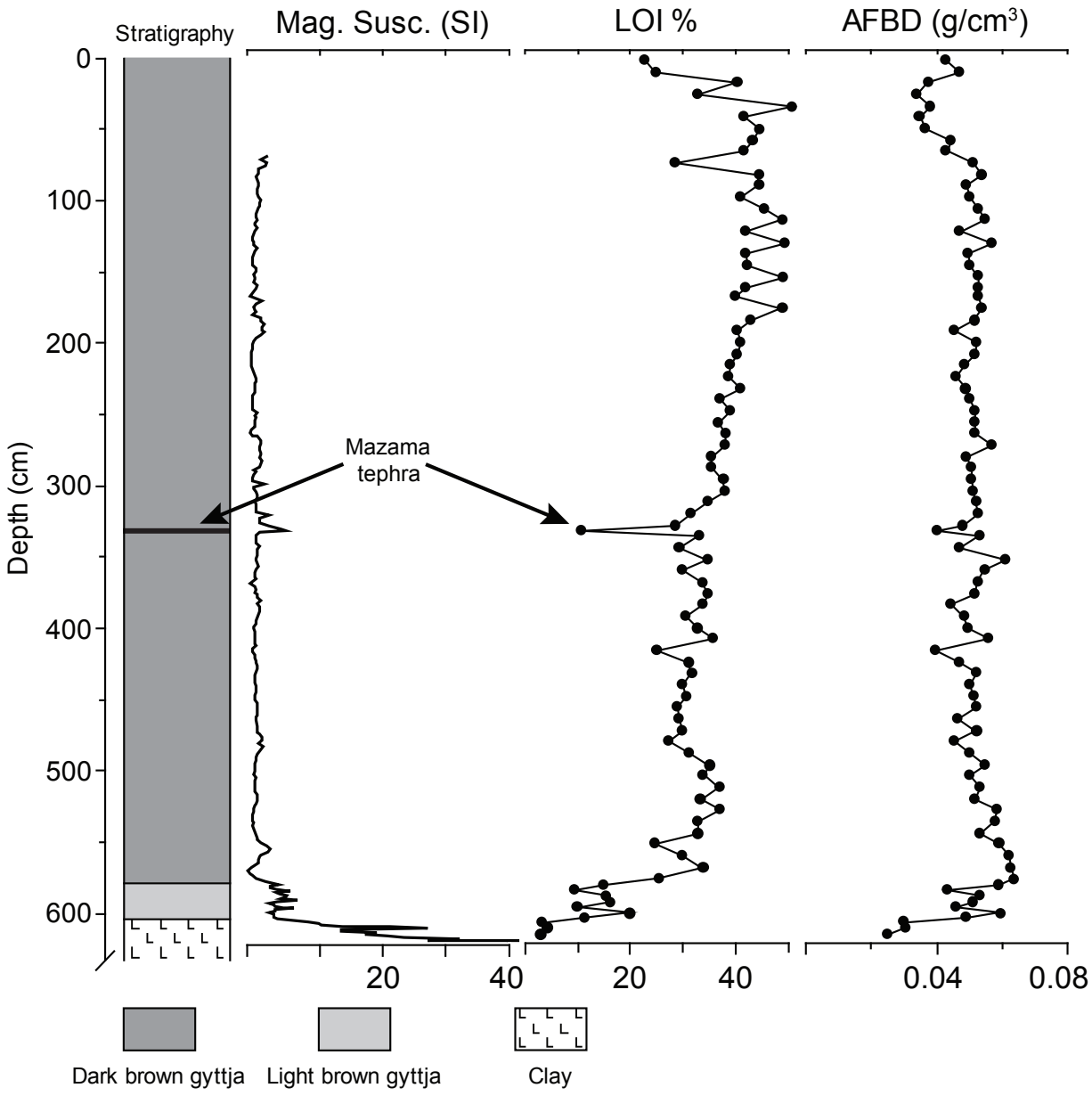
Stratigraphy
Mag. Susc. (SI)
LOI %
AFBD (g/cm3)
Depth (cm)
0
100
200
300
400
500
600
Mazama
tephra
20
40
20
40
0.04
0.08
Dark brown gyttja
Light brown gyttja
Clay

Figure 3

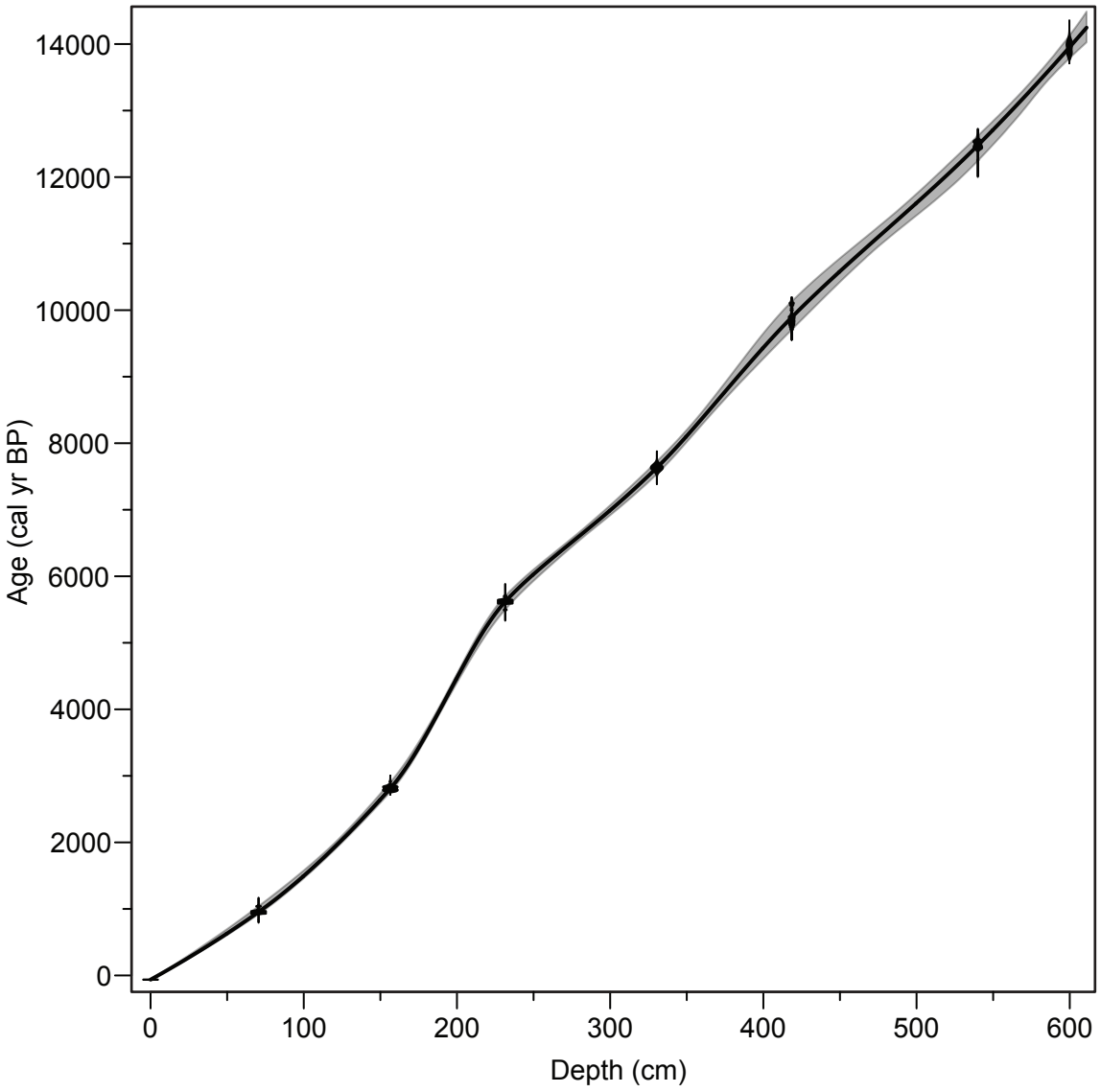
14000
12000
10000
8000
6000
4000
2000
0
Age (cal yr BP)
0
100
200
300
400
500
600
Depth (cm)

Figure 4

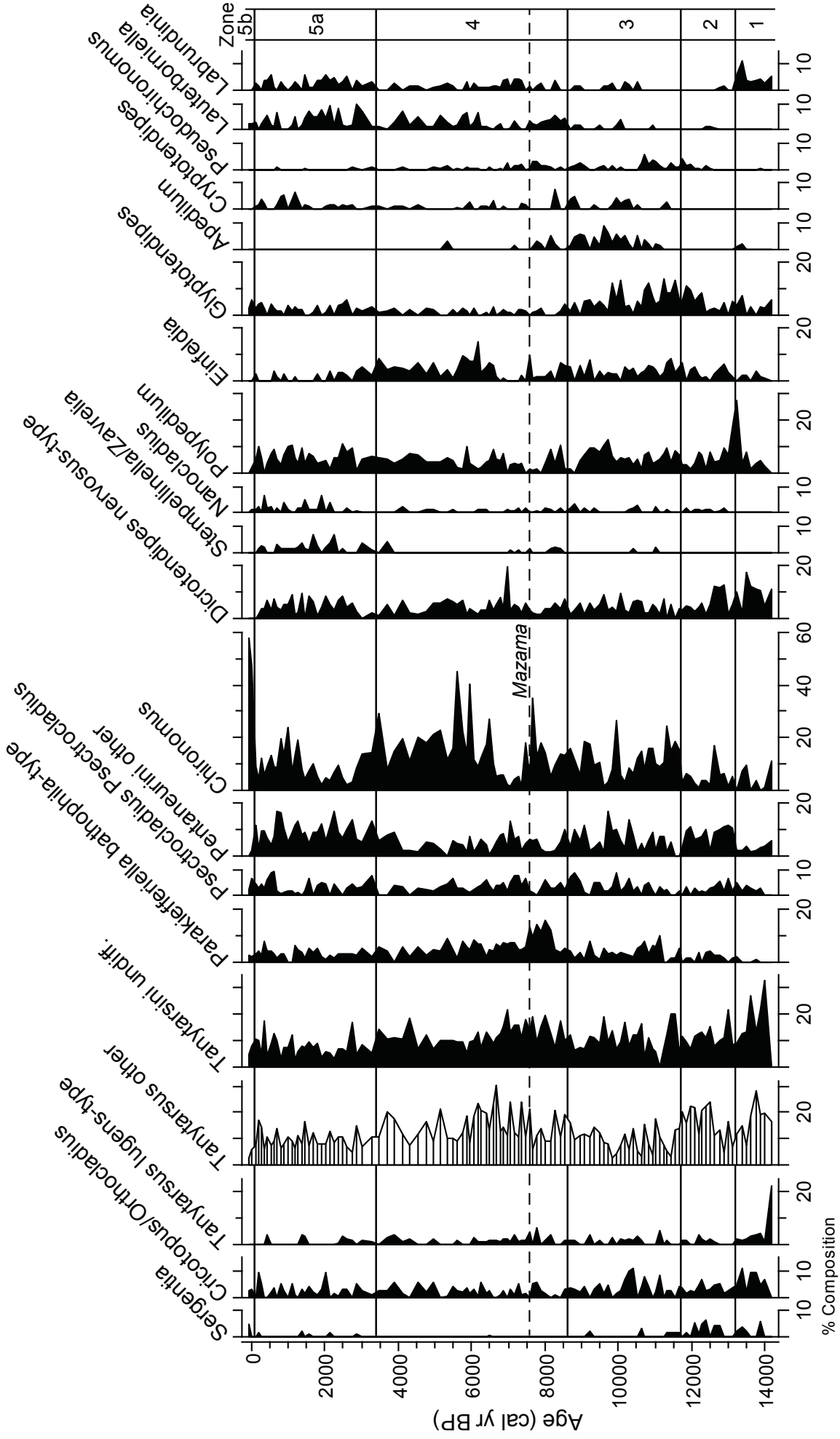
Zone
5b
5a
4
3
2
1
Age (cal yr BP)
0
2000
4000
6000
8000
10000
12000
14000
% Composition
Mazama
Sergentia
Cricotopus/Orthocladius
Tanytarsus lugens-type
Tanytarsus other
Tanytarsini undiff.
Parakiefferiella bathophila-type
Psectrocladius Psectrocladius
Pentaneurini other
Chironomus
Dicrotendipes nervosus-type
Stempellinella/Zavrelia
Nanocladius
Polypedilum
Einfeldia
Glyptotendipes
Apedilum
Cryptotendipes
Pseudochironomus
Lauterborniella
Labrundinia

Figure 5

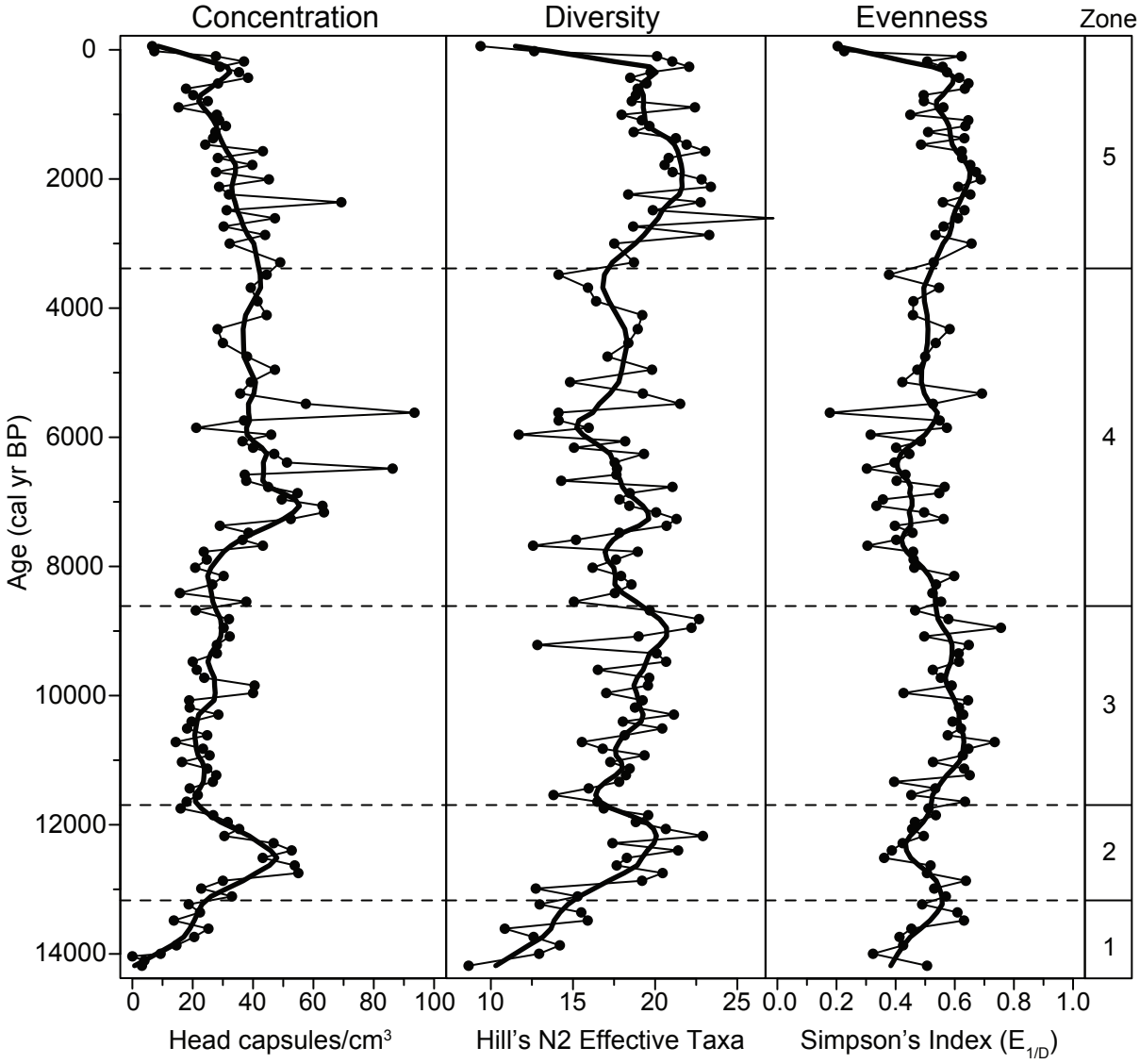
Concentration
Diversity
Evenness
Zone
Age (cal yr BP)
0
2000
4000
6000
8000
10000
12000
14000
5
4
3
2
1
0 20 40 60 80 100
Head capsules/cm3
10 15 20 25
Hill's N2 Effective Taxa
0.0 0.2 0.4 0.6 0.8 1.0
Simpson's Index (E1/D)

Figure 6

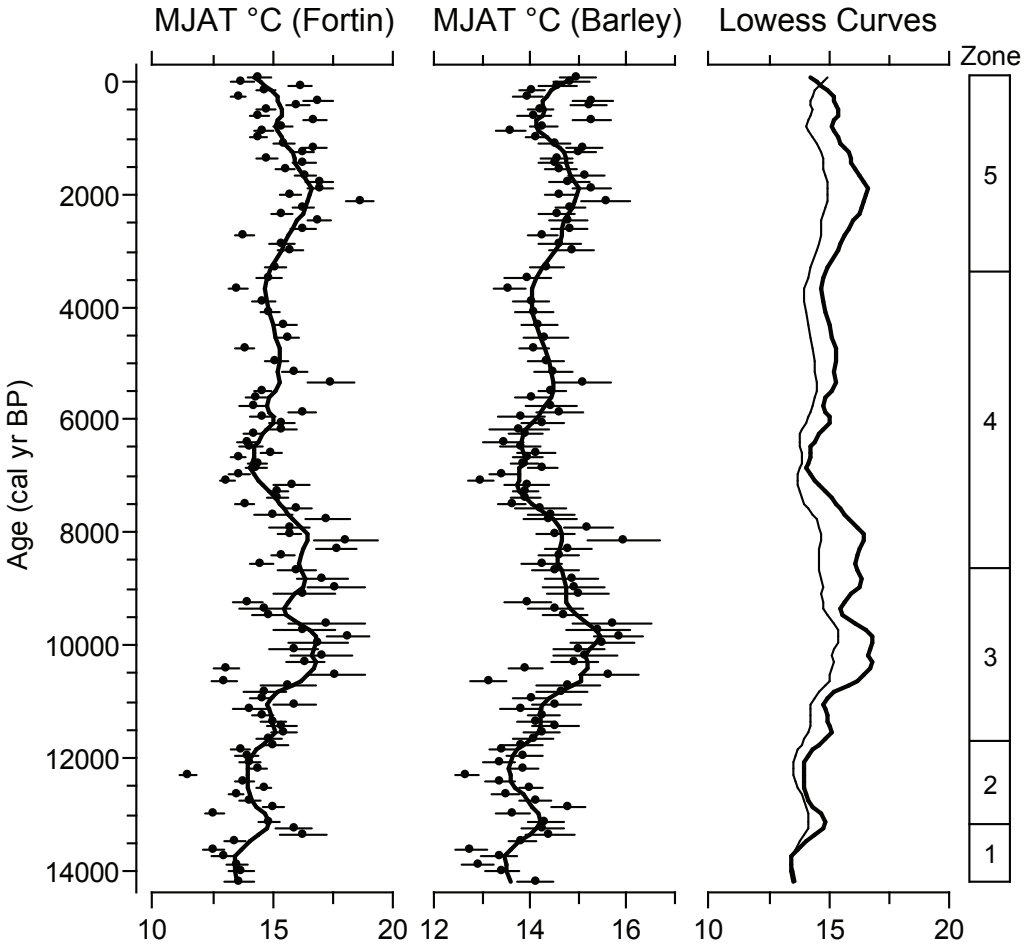
MJAT °C (Fortin)
MJAT °C (Barley)
Lowess Curves
Zone
Age (cal yr BP)
0
2000
4000
6000
8000
10000
12000
14000
10
15
20
12
14
16
10
15
20
5
4
3
2
1

Figure 7

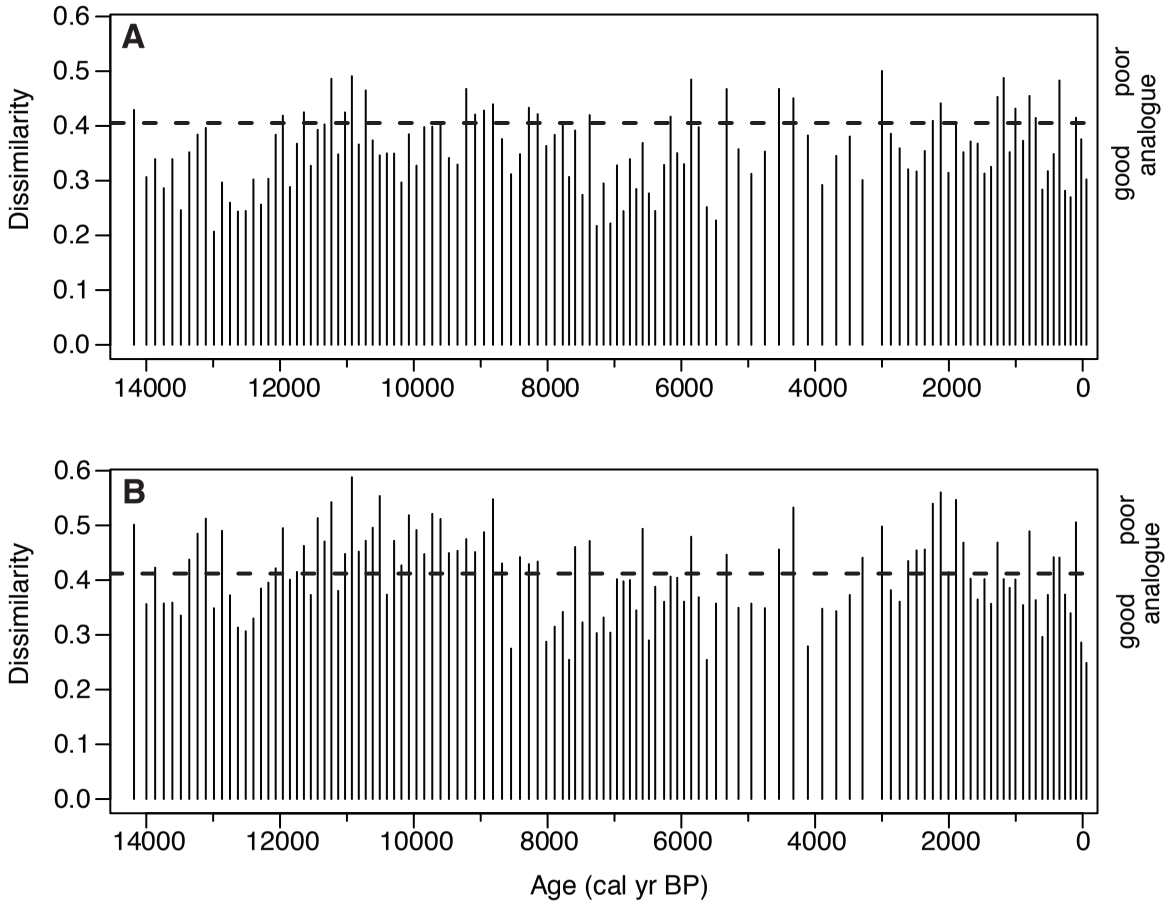
A
Dissimilarity
0.6
0.5
0.4
0.3
0.2
0.1
0.0
poor
good analogue
14000
12000
10000
8000
6000
4000
2000
0

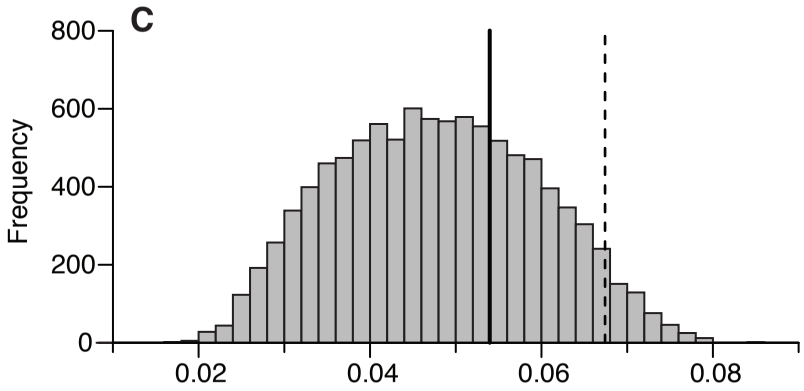
C
Frequency
800
600
400
200
0
0.02
0.04
0.06
0.08

B
Dissimilarity
0.6
0.5
0.4
0.3
0.2
0.1
0.0
poor
good analogue
14000
12000
10000
8000
6000
4000
2000
0
Age (cal yr BP)

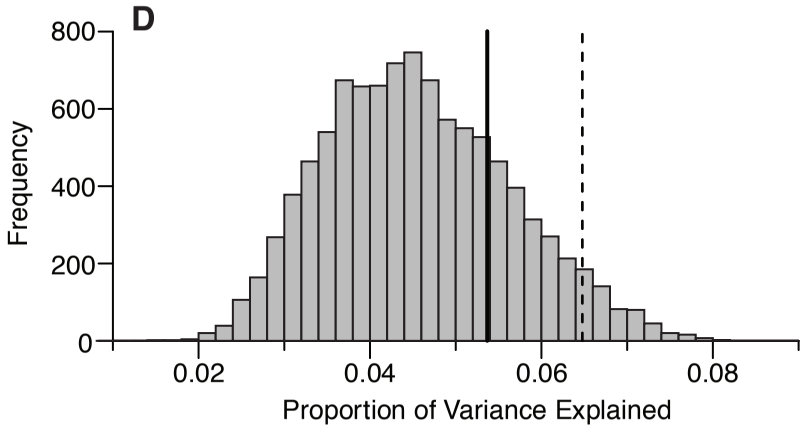
D
Frequency
800
600
400
200
0
0.02
0.04
0.06
0.08
Proportion of Variance Explained

Figure 8

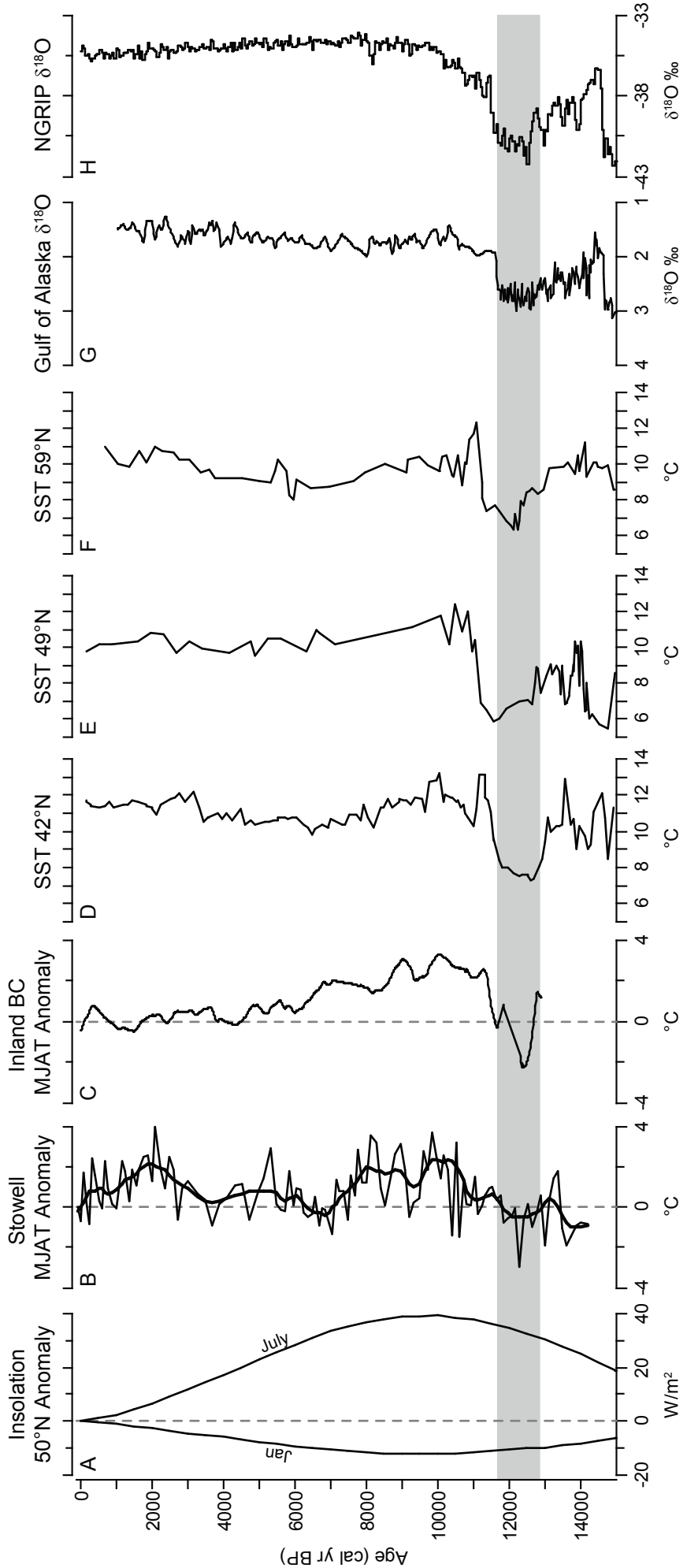
Insolation 50°N Anomaly
A
July
Jan
W/m²
Stowell MJAT Anomaly
B
°C
Inland BC MJAT Anomaly
C
°C
SST 42°N
D
°C
SST 49°N
E
°C
SST 59°N
F
°C
Gulf of Alaska δ18O
G
δ18O ‰
NGRIP δ18O
H
δ18O ‰
Age (cal yr BP)

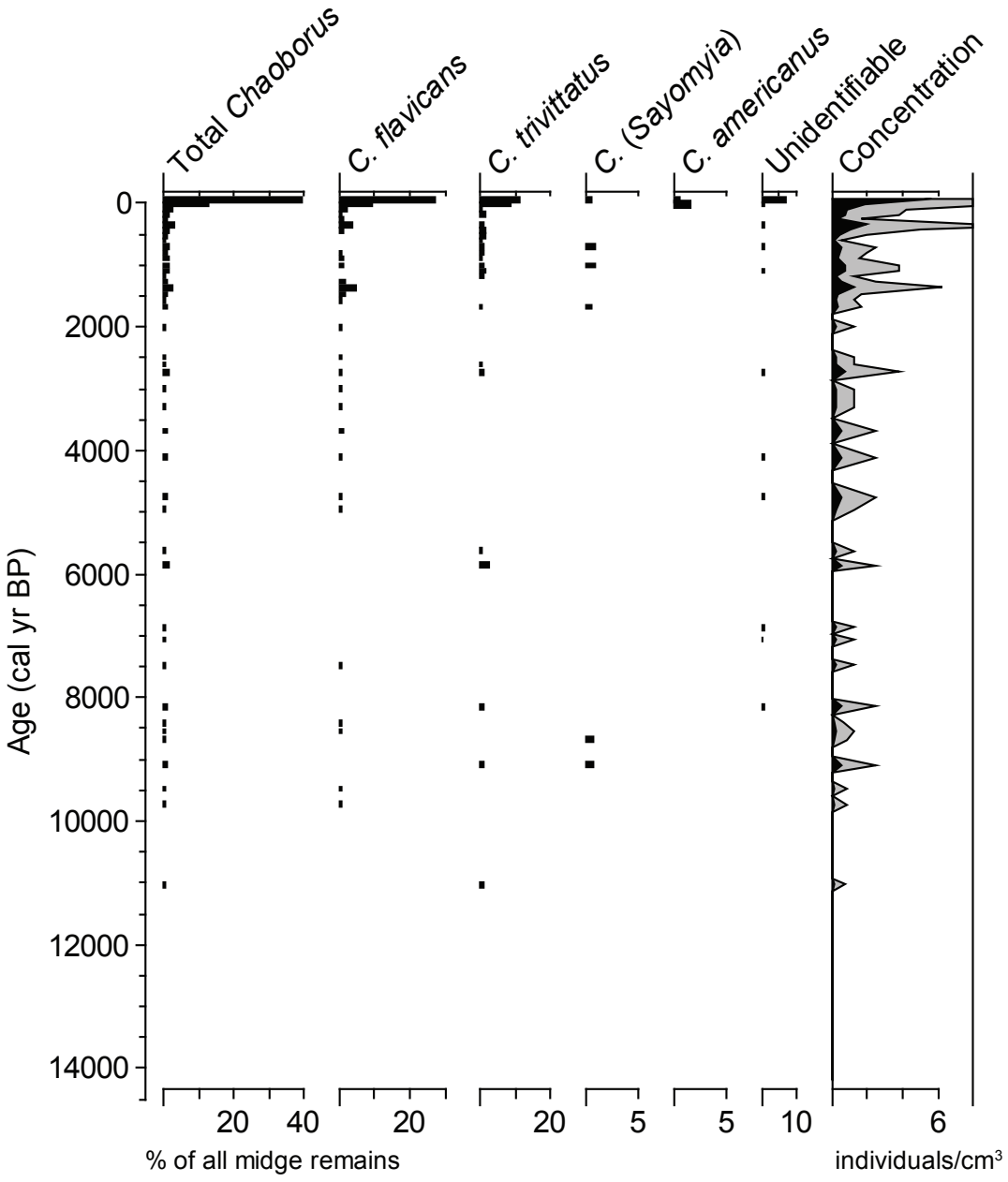

Electronic Supplementary Material Fig. S1 *Chaoborus* percentages and total concentration (individuals/cm^3) in the sediment core from Lake Stowell, Saltspring Island, British Columbia. Each *Chaoborus* mandible was counted as half of one individual. Note changes in scale for *C.* (*Sayomyia*) and *C. americanus*. Grey shading represents 5× exaggeration